Biointerphases (2012) 7:34
DOI 10.1007/s13758-012-0034-x

ARTICLE

Response of Osteoclasts to Titanium Surfaces with Increasing Surface Roughness: An In Vitro Study

Jenny Brinkmann · Thomas Hefti · Falko Schlottig · Nicholas D. Spencer · Heike Hall

Received: 30 March 2012 / Accepted: 23 April 2012 / Published online: 25 May 2012

Abstract Osteoclasts are responsible for bone resorption and implant surface roughness promotes osseointegration. However, little is known about the effect of roughness on osteoclast activity. This study aims at the characterization of osteoclastic response to surface roughness. The number of osteoclasts, the tartrate-resistant acid phosphatase and matrix metalloproteinase (MMP) activities, the cell morphology and the actin-ring formation were examined on smooth (TS), acid-etched (TA) and sandblasted acid-etched (TLA) titanium and on native bone. Cell morphology was comparable on TA, TLA and bone, actin rings being similar in size on TLA and bone, but smaller on TA and virtually absent on TS. Gelatin zymography revealed increased proMMP-9 expression on TA, TLA, and bone compared to TS. In general, osteoclasts show similar characteristics on rough titanium surfaces and on bone, but reduced activity on smooth titanium surfaces. These results offer some insight into the involvement of osteoclasts in remodeling processes around implant surfaces.

Deceased: Heike Hall.

J. Brinkmann · T. Hefti (✉) · H. Hall
Cells and BioMaterials, Department of Materials, ETH Zurich,
Wolfgang-Pauli-Strasse 10, 8093 Zürich, Switzerland
e-mail: hefti.thomas@gmail.com

J. Brinkmann
e-mail: j.brinkmann@utwente.nl

Present Address:
J. Brinkmann
Molecular Nanofabrication, MESA+ Institute for
Nanotechnology, University of Twente,
P.O. Box 217, 7500 AE Enschede, The Netherlands

T. Hefti · N. D. Spencer
Laboratory for Surface Science and Technology,
Department of Materials, ETH Zurich,
Wolfgang-Pauli-Strasse 10, 8093 Zürich, Switzerland
e-mail: nspencer@ethz.ch

T. Hefti · F. Schlottig
Thommen Medical, Hauptstrasse 26 d,
4437 Waldenburg, Switzerland
e-mail: falko.schlottig@thommenmedical.com

1 Introduction

Bone is a highly dynamic tissue that is constantly being remodeled, in order to regulate its architecture to satisfy mechanical needs, and to repair damaged tissue [1]. Initiation of the remodeling cycle is achieved by the activation of osteoclasts, which resorb the underlying bone tissue, and followed by subsequent activation of osteoblasts, which are responsible for formation of new bone tissue. The successful integration of an implant in bone tissue, so-called osseointegration, is accomplished by bone remodeling around the implant site [2]. This remodeling process requires a balanced activation of osteoclasts and osteoblasts to form new and healthy bone tissue in the peri-implant region [3–5]. Certain implant properties, such as surface roughness, influence osteoblast proliferation as well as differentiation and positively affect the successful integration of the implant [4, 6, 7]. Although a balanced stimulation of osteoclasts is required for adequate bone remodeling in the peri-implant region, the effect of implant surface roughness on osteoclast behavior has not been widely addressed. Osteoclasts have been shown to sense topographical changes on a nanometer scale, measured as changes in tartrate-resistant acid phosphatase (TRAP) activity [8, 9] as well as sealing zone (SZ) assembly and stability [10, 11]. On the micrometer scale, topographical roughness of hydroxylapatite increased both TRAP activity

and gene-expression levels of osteoclastic genes with increased roughness [12]. Additionally, micro-roughened titanium was shown to increase mRNA levels of osteoclast-differentiation markers [13], and the number of differentiated osteoclasts [4] increased from smooth to rough surfaces. In general, micrometer-scale surface roughness has been widely recognized to lead to improved osseointegration [3]; however, the effects of different surface morphologies on osteoclast activation and adhesion as well as a comparison of the results with the behavior of native bone remain to be investigated.

Activated mature osteoclasts are polarized multinucleated cells that form specialized adhesive structures, podosomes, formed by F-actin, which essentially mature into the sealing zone (SZ) [14, 15], and bind the cell tightly to the bone surface. SZs are microscopically visible as ring-like actin structures near the interface of the cell to the substrate surface and its complete assembly is essential for bone resorption [16]. A specialized membrane domain is created within the SZ, the ruffled border (RB) [17]. In the SZ the pH is lowered through protons of vacuolar H^+-ATPase released through the RB, dissolving the mineral phase, which is mainly composed of hydroxylapatite [18]. Additionally proteolytic enzymes, such as matrix metalloproteinases (MMPs) and cathepsin K, which are responsible for cleavage and degradation of the organic bone matrix, are released through the RB into the SZ. MMPs are secreted as inactive proMMPs and require an activation step in order to cleave extracellular matrix (ECM) proteins. Activation of MMPs depends on the disruption of a bond formed by cysteine residue Cys^{73} and an active Zn^{2+} site, and this is usually performed by other proteinases. Cleavage of the pro-domain causes a mass reduction of the pro-enzyme by 8–10 kDa [19, 20]. The presence of these proteolytic enzymes in activated osteoclasts can be assessed by gelatin zymography [21, 22]. Activated osteoclasts express the enzyme TRAP, which is also an important marker molecule for osteoblast activation [23–25]. For in vitro studies of osteoclasts and as an alternative to primary cells, the murine pre-osteoclast cell line RAW 264.7, differentiated by the addition of Receptor Activator of NF-κB ligand (RANKL), is a recognized model and has been reported to generate characteristics of a fully differentiated osteoclast, such as polarized morphology of multinucleated cells, actin ring formation, TRAP activity and resorption of bone [26, 27].

To the best of our knowledge, a detailed in vitro study of osteoclasts cultured on titanium surfaces with increasing surface roughness on the micrometer scale, with respect to cell morphology, differentiation, adhesion and activation has not been described previously. In addition to confocal laser scanning microscopy (CLSM) to study cell adhesion, morphology and actin ring formation, scanning electron microscopy (SEM) was employed to observe the interaction of the cells with the different surfaces. As a marker for differentiation, TRAP activity was measured and the resorption potential of the cells assessed by analyzing MMP activity with gelatin zymography. Characterizing osteoclast response on titanium surfaces with increasing roughness in the micrometer range, identical or similar to implant surfaces, might offer further understanding of the bone remodeling processes near implant surfaces.

2 Materials and Methods

2.1 Preparation of Bone Slices

Bone slices from bovine femurs were prepared as previously described [28]. In brief, slices with a thickness of approximately 0.5 mm were sawn from cortical bone cylinders with a diameter of approximately 10 mm. Immersion in 70 % ethanol for 24 h at 4 °C, rinsing and additional 24 h immersion in phosphate-buffered saline (PBS; Sigma-Aldrich, Buchs, Switzerland) with 1 % antibiotic–antimycotic solution (ABAM) (Invitrogen, Carlsbad, CA, USA) was used for sterilization of the bone slices. The slices were stored at −80 °C until use, when they were washed twice in PBS at room temperature prior to use.

2.2 Titanium Surfaces

Smooth titanium surfaces (TS) were prepared from silicon wafers coated with 40 nm of titanium (Paul Scherrer Institute, Villigen, Switzerland) and cut into squares of 8 × 8 mm. Rough titanium surfaces were prepared as previously described [28]. Disks made out of titanium grade 4 (Thommen Medical, Waldenburg, Switzerland) with a diameter of 15 mm were treated by sandblasting with alumina particles with sizes of 126–150 μm followed by hot-acid etching in a solution of hydrochloric acid (14 %) and sulfuric acid (34 %) (TLA) and only hot-acid etching (TA) (Table 1). Surface roughness (S_a) was measured with optical confocal profilometry (Plu NeoX, Sensofar, Terassa, Spain), data were analyzed with the SensoMap software (Sensofar, Terassa, Spain). Prior to cell

Table 1 Overview of surface treatments and surface roughness (S_a) for titanium surfaces

Short name	Treatment	S_a (μm)
TS	None	$(2.1 \pm 0.1) \times 10^{-3}$
TA	Hot acid etched	1.33 ± 0.05
TLA	Sandblasted and hot acid etched	2.60 ± 0.30

seeding, samples were sterilized in 70 % ethanol and thereafter rinsed twice in PBS.

2.3 Cell Culture

Murine RAW 264.7 (TIB-71; ATCC) macrophage monocytes were cultured in 5 % CO_2 at 37 °C in α-MEM medium without phenol red (Invitrogen, Carlsbad, CA, USA) containing 10 % heat-inactivated fetal bovine serum (FBS; Invitrogen, Carlsbad, CA, USA) and 1 % ABAM. Cells were seeded at an initial density of 2,000 cells/cm^2 in the presence of 50 ng/ml mouse RANKL (Invitrogen, Carlsbad, CA, USA) and were cultured for 11 days. Medium and RANKL were exchanged every 2–3 days. At day 9 cells were washed twice in PBS and for the last 48 h they were cultured in serum-free medium, supplemented with 300 μg/ml bovine serum albumin (BSA), 100 μg/ml human apotransferrin, 1 μg/ml insulin and 160 ng/ml selenium (all from Sigma-Aldrich, Buchs, Switzerland). The medium was removed after 11 days, the cells were lysed, and the lysate was incubated on ice for 1 h while vortexing every 10 min and centrifuged at 15,000*g* for 20 min at 4 °C. Supernatants were collected and stored at −20 °C until use.

2.4 Picogreen DNA Assay

DNA was measured using the fluorescent nucleic acid stain Picogreen (Quant-iT™ PicoGreen dsDNA Kit; Invitrogen, Carlsbad, CA, USA) according to the manufacturer's instructions. 10 μl of lysate were diluted 1:10 in TE buffer (10 mM TRIS, 1 mM EDTA; pH 7.5) and added to 100 μl of colorimetric dye solution. After 5 min incubation at room temperature, samples were excited at 480 nm and emission was read at 520 nm using a microplate reader (Tecan Infinite M200, Männedorf, Switzerland).

2.5 TRAP Assay

TRAP activity was measured using a commercially available TRAP-staining kit (Kamiya Biomedical Company, Seattle, WA, USA). In brief, 15 μl of cell lysate were diluted in 85 μl of chromogenic substrate and incubated for 3 h at 37 °C. Readout of optical density at 540 nm was performed with a microplate reader. Additionally, TRAP-staining was performed on fixed cells, to confirm that all cells having more than three nuclei, which were identified as osteoclasts, appeared to be TRAP-positive.

2.6 CLSM Analysis

After 11 days of culture, cells were washed twice in PBS, fixed in 4 % paraformaldehyde (Sigma-Aldrich, Buchs, Switzerland) for 10 min at room temperature, washed three times with PBS, permeabilized in PBST (0.25 % Triton X-100 in PBS) for 10 min, washed three times with PBS and blocked with 2 % BSA in PBS for 1 h at room temperature. The actin cytoskeleton was stained with phalloidin (Alexa Fluor 488 phalloidin; Invitrogen, Carlsbad, CA, USA) 1:100 in PBS for 1 h, and cell nuclei were stained with DAPI (Invitrogen, Carlsbad CA, USA) 1:1,000 in PBS, for 15 min. Using CLSM (Leica SP5, Wetzlar, Germany), samples were imaged at three different spots each. 20× magnification was used for counts of multinucleated osteoclasts (cells having more than three nuclei) and determination of osteoclast size. 63× magnification (water immersion) was used for measurements of actin ring size. Images were analyzed using ImageJ 1.44p software (National Institutes of Health, Bethesda, MD, USA).

2.7 SEM

Cells were fixed with 2 % glutaraldehyde in PBS for 10 min at room temperature after 11 days of culture, followed by staining in 2 % osmium tetroxide in PBS for 20 min and dehydrated in an ascending ethanol series. After critical-point drying, (CPD 30, Baltec, Liechtenstein), samples were sputter-coated with 6 nm platinum (SCD500, Baltec, Liechtenstein) and then examined in the SEM (Zeiss, SUPRA 50 VP, Germany).

2.8 Gelatin Zymography

Total protein concentrations in cell lysates and supernatants were determined using a BSA standard assay (Pierce BCA Protein assay kit, Thermo Scientific, Waltham, MA, USA). For that purpose 25 μl of diluted standard and sample (1:10 in PBS) were added to 200 μl of colorimetric working reagent and incubated for 30 min at 37 °C. Optical density was read at 562 nm using a microplate reader. 8 % polyacrylamide gels were co-polymerized with 1 mg/ml gelatin (Type A: from porcine skin, Sigma-Aldrich, Buchs, Switzerland). Separation of 750 μg protein/lane was done under non-reducing conditions on ice. Purified MMP-2 and proMMP-9 (Chemicon, Billerica, MA, USA) were used as positive controls. Subsequent renaturing of the protein was carried out by 30 min incubation in freshly prepared 2.5 % Triton X-100 solution followed by incubation in enzyme activation buffer (50 mM TRIS–HCl, 200 mM NaCl, 5 mM CaCl; pH 7.5) overnight at 37 °C where the buffer was exchanged after the first 30 min. Subsequently gels were washed in ddH_2O, stained in 0.1 % Coomassie Blue solution (50 % methanol, 10 % acetic acid, 0.1 % brilliant Blue R250 in ddH_2O) for 2 h and destained for 20 min in destaining solution (10 % acetic acid; 20 % ethanol in ddH_2O). Visualization and photo documentation of the gels were carried out with a gel scanner (Witec AG, Littau, Switzerland).

2.9 Statistics

For DNA and TRAP analysis, three independent experiments were performed, each in triplicate. Results were expressed as mean ± standard deviation (SD). One-way ANOVA with a Tukey post hoc test was used to compare the means among groups. Due to the asymmetrical distribution of data for cell size and actin ring size a Kruskal–Wallis non-parametric ANOVA was used. The different groups were compared with a Mann–Whitney post hoc test including Bonferroni correction. OriginLab 8.0 (Northampton, MA, USA) was used for calculation, and statistical significance levels were set at $p < 0.05$ (*) and $p < 0.01$ (**) for both tests.

3 Results

3.1 Cell Number and Differentiation

To assess cell number of cells grown on the different surfaces, DNA content was measured after 11 days of culture. As shown in Fig.1a DNA content was significantly higher for cells grown on smooth surfaces (TS), with almost double the amount of DNA compared to rough titanium surfaces (TA and TLA) and about three times the DNA content measured on bone (both $p < 0.01$). Furthermore, DNA content was significantly higher on TLA and TA compared to bone ($p < 0.05$).

TRAP activity was determined and normalized to DNA content to assess osteoclast differentiation (Fig. 1b). The highest TRAP activity was found on bone, which was significantly different from smooth and rough titanium surfaces ($p < 0.01$). Additionally, cells on TS showed an increased TRAP activity compared to cells grown on the rough TLA ($p < 0.01$) and TA ($p < 0.05$). Control experiments showed no TRAP activity from the bone slices alone (data not shown).

As an additional measure to evaluate osteoclast differentiation, the number of osteoclasts, defined as cells with more than three nuclei, was counted on the different substrates (n = 21 images per surface) (Fig. 1c). Although TS showed a higher TRAP activity compared to that determined for TA and TLA, a greater number of osteoclasts was found on these rough titanium surfaces compared to the smooth TS ($p < 0.05$). However, most osteoclasts were

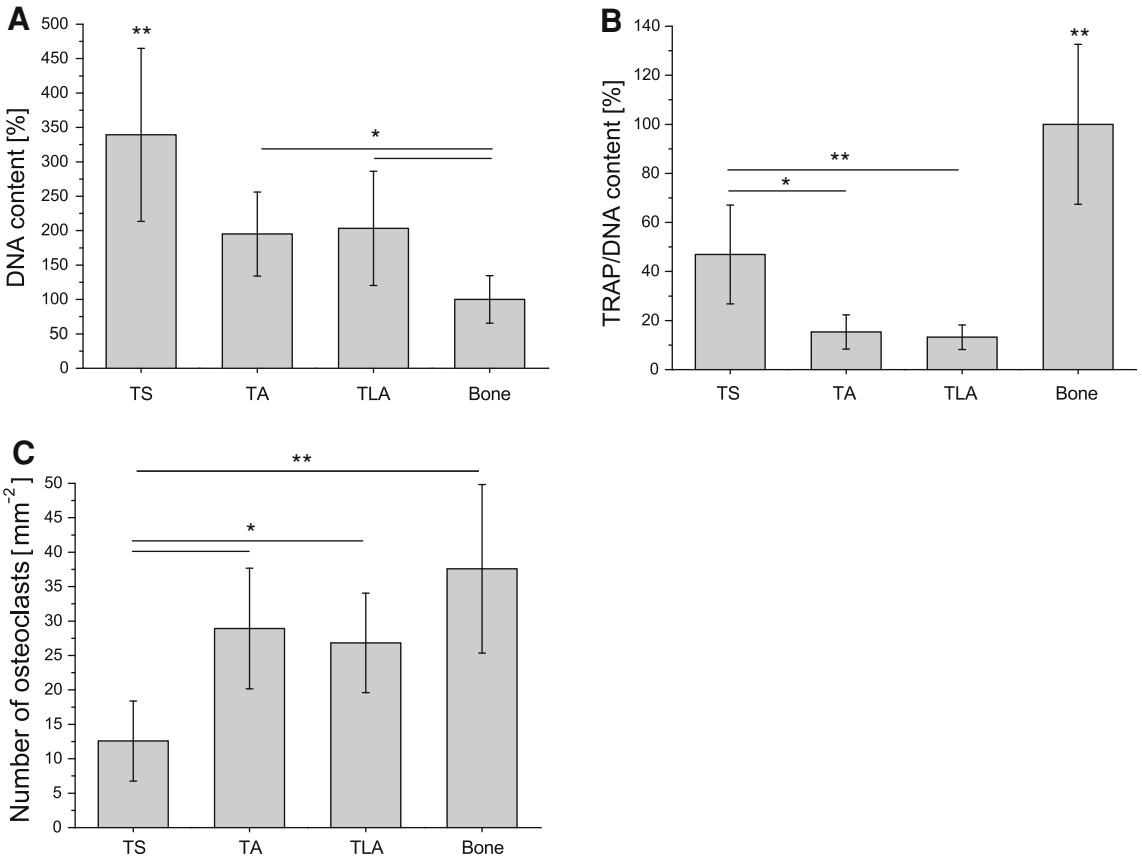

Fig. 1 DNA content (**a**), specific enzymatic TRAP activity (**b**) and cell count of differentiated osteoclasts (**c**) cultured on TS, TA, TLA and bone. Data in **a** and **b** were normalized to bone (100 %) and represent means ± SD of three independent experiments. Statistically significant differences are indicated with $p < 0.05$ (*) and $p < 0.01$ (**)

found on bone, which was significantly different from TS ($p < 0.01$) but not from TA and TLA. No significant differences between TA and TLA were observed in any of the three assays.

3.2 Qualitative Image Analysis of Osteoclast Morphology and Adhesion

For the investigation of osteoclast adhesion and morphology by immunostaining cells were stained for F-actin (cytoskeleton) and DNA (cell nuclei) to reveal morphological differences between osteoclasts grown on different substrates. In Fig. 2, representative images show typical adhesion structures formed by osteoclasts. Podosomes are osteoclastic adhesion structures primarily found in premature osteoclasts, appearing as dot-like cylindrical actin assemblies. Podosomes may turn into actin rings [14], forming the core of the sealing zone in activated osteoclasts. Cells cultured on TS (Fig. 2a) showed extensive podosome formation, whereas cells cultured on bone predominantly formed actin rings (Fig. 2b). Filopodia formation occurred with different characteristics. On TS, osteoclasts typically showed multiple filopodia extending from the entire cell membrane whereas, on bone, filopodia were scarce, occurring in randomly distributed clusters.

A comparison of characteristic cell morphology and adhesion structures on all the investigated surfaces is presented in Fig. 3, as visualized by CLSM and SEM. Differences were primarily related to cell size, as well as the formation and size of actin rings. Osteoclasts on TS had a flat appearance and the tendency to form multinucleated giant cells (Fig. 3a, b). Formation of actin rings was rarely observed on these surfaces, instead a large number of podosomes and formation of a podosome belt was almost exclusively found in cells cultured on these surfaces (Fig. 3a). An additional characteristic for these smooth TS surfaces was the large number of filopodia extending from the cell membrane, adhering the cell to the underlying substrate (Fig. 3c). Osteoclasts on both rough titanium surfaces showed a similar distribution of multinucleated cells, similar cell morphology and similar formation of the numerous actin rings (Fig. 3d–i). Differences between them were related to actin ring size, those on TLA being generally bigger than those on TA. Magnified SEM images of TA and TLA showed similar tight adhesion structures of osteoclasts grown on these rough surfaces (Fig. 3f, i), however fewer filopodia were visible on the rough surfaces than on the smooth surface.

Osteoclasts on bone were generally larger in size than those found on rough surfaces (Fig. 3j–l), but did not extend to sizes as seen on TS. Analogous to the rough surfaces, a large number of actin rings could be observed (Fig. 3j) as well as a tight adhesion of osteoclasts with the bone surface (Fig. 3l). Here, a remarkable amount of exposed collagen fibrils could be observed across the bone surface (Fig. 3k, l), showing extensive resorptive activity of osteoclasts cultured on bone.

3.3 Quantitative Image Analysis of Cell Morphology and Adhesion

The size of multinucleated cells was measured for all surfaces ($n > 180$ cells per surface) (Fig. 4). Significant differences were observed between all the groups ($p < 0.05$). Cells cultured on TS showed the widest range in size compared to osteoclasts grown on rough titanium surfaces and on bone (Table 2). With increasing surface roughness the osteoclasts decreased in size on TLA compared to TA. However, osteoclasts cultured on bone were larger than those found on the rough titanium surfaces. Actin rings were measured on TA, TLA and bone for quantitative comparison ($n = 100$ actin rings per surface) (Fig. 5). Only closed actin rings with a clearly visible contour were included in the analysis, actin ring size being

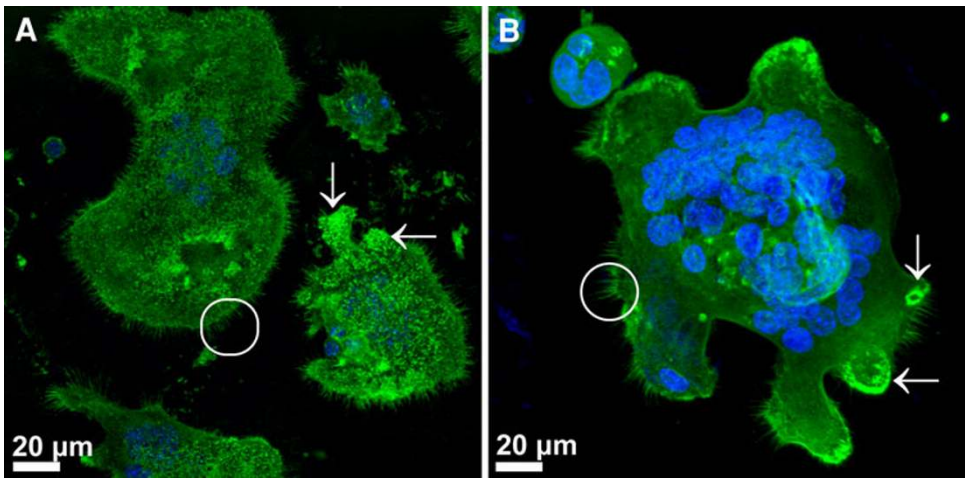

Fig. 2 Morphology of osteoclast adhesions structures. Confocal micrographs of differentiated osteoclasts immunostained for F-actin (*green*) and cell nuclei (*blue*) on TS (**a**) and bone (**b**). Osteoclasts showed formation of podosomes (mainly on TS) and actin ring formation (here exemplary shown on bone), both indicated with *white arrows*. *White circles* indicate filopodia extending from the cell periphery

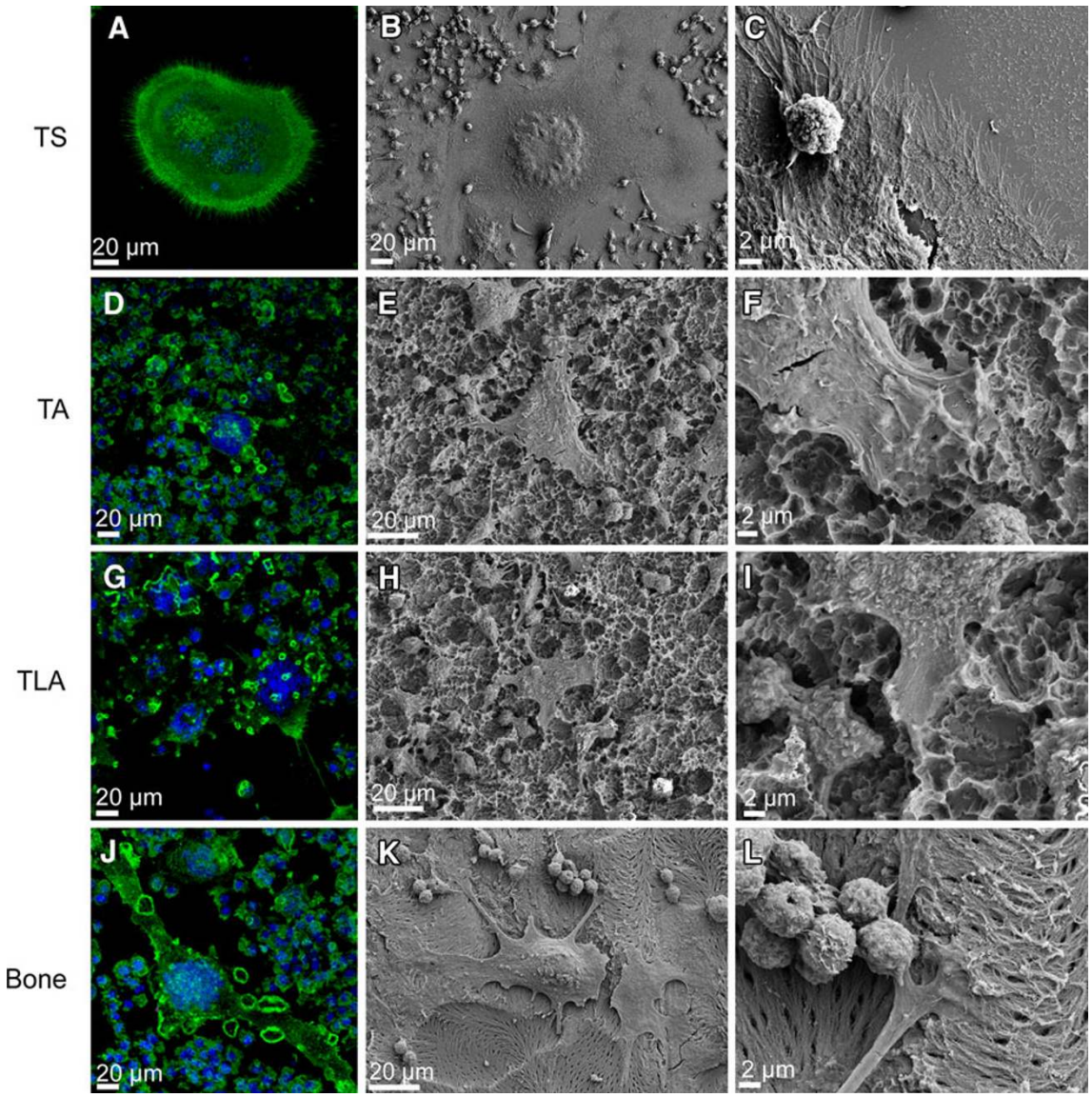

Fig. 3 Confocal (*left column*) and SEM (*middle* and *right column*) micrographs of differentiated osteoclasts cultured on TS, TA, TLA and bone. For confocal microscopy cells were immunostained for F-actin (*green*) and cell nuclei (*blue*). On TS a podosome belt and multiple filopodia extending from the cell periphery could be observed (**a**–**c**). Osteoclast morphology as observed in confocal microscopy was fairly similar for TA and TLA (**d**, **g**), osteoclasts cultured on bone showed the same characteristics but were bigger and showed bigger actin rings (**j**). In SEM cell attachment to the surface could be visualized. Cells cultured on TA (**e**, **f**), TLA (**h**, **i**) and bone (**k**, **l**) had a similar morphology; they formed elongated cytoplasmic extensions to attach to the underlying surface. On bone resorbed areas with loose collagen fibers became visible (**l**)

defined as the maximal width measured. On TS, actin rings occurred rarely and could not be used for a meaningful analysis. Osteoclasts on TA exhibited actin rings ranging from 1.7 to 9.5 µm having a median of 4.3 µm, but they were significantly smaller than actin rings on TLA and bone ($p < 0.05$). No significant difference was seen between the size of actin rings on bone (1.1 – 28.2 µm; median 6.6 µm) and on TLA (2.0 – 24.8 µm; median 5.5 µm). Both the largest and smallest actin ring was measured on bone, where the widest range of actin rings was found.

3.4 Gelatin Zymography

To assess MMP activity of osteoclasts, gelatin zymography was performed with cell lysates and supernatants. The presence of proMMP-9 could be confirmed in all samples, as illustrated in Fig. 6 with a characteristic example. However, the intensity of the signal, and hence the concentration of synthesized enzyme in the sample, differed between the surfaces. On TS, the signal had a very low intensity compared to those on TA, TLA and bone. Conversely, no significant differences were detected between

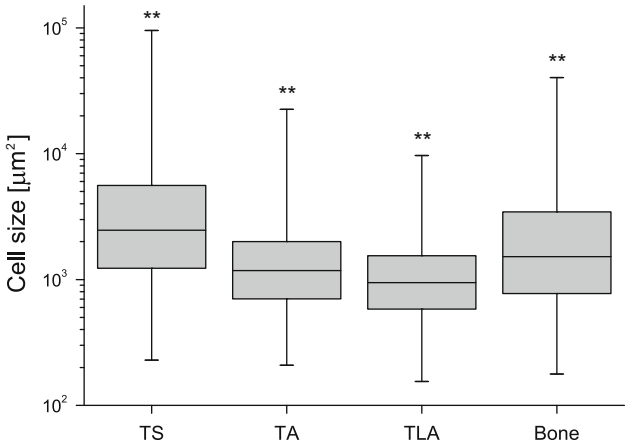

Fig. 4 Cell size of differentiated osteoclasts cultured on TS, TA, TLA and bone. Data represent the respective minima, first quartile, median, third quartile and maxima of cell size, obtained from measurements of $n > 180$ cells for each surface in three independent experiments. Statistically significant differences between the substrates are indicated with $p < 0.01$ (**)

Table 2 Cell size on all investigated surfaces of differentiated osteoclasts expressed in median, first and third quartile, Q_1 and Q_3, minimum and maximum values

Substrate	*n*	Cell size (µm²)				
		Min	Q_1	Median	Q_3	Max
TS	182	228	1,235	2,464	5,560	95,058
TA	414	208	703	1,179	2,000	22,524
TLA	346	155	583	946	1,543	9,647
Bone	538	177	778	1,521	3,435	40,200

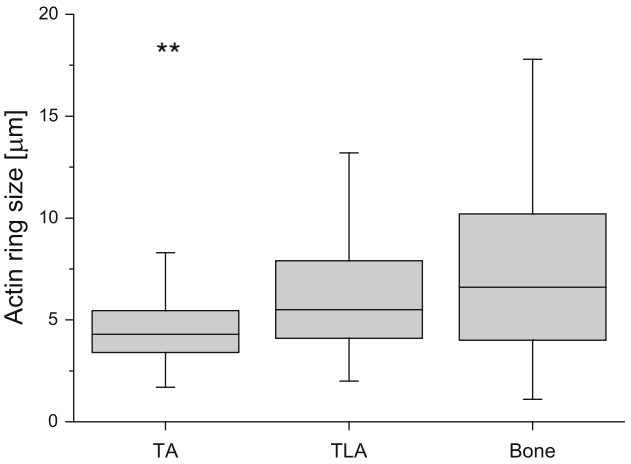

Fig. 5 Actin ring size of differentiated osteoclasts on TA, TLA and bone illustrated as *box plots*. On TS no actin rings were found. Data represent the respective minima, first quartile, median, third quartile and maxima of actin ring size, obtained from measurements of $n > 100$ actin rings for each surface in three independent experiments. Statistically significant differences between the substrates are indicated with $p < 0.01$ (**)

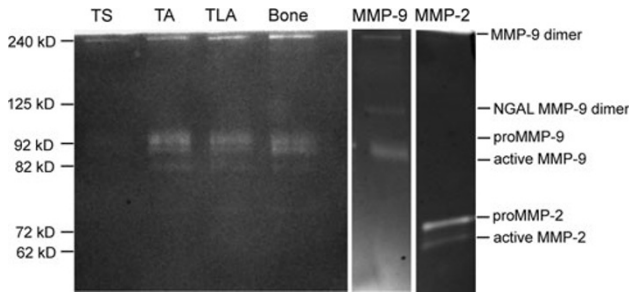

Fig. 6 Gelatin zymography with cell lysates of differentiated osteoclasts cultured on TS, TA, TLA and bone. Clear bands of proMMP-9 and active MMP-9, as well as weak bands of proMMP-2 were visible for TA, TLA and bone. On TS only a weak signal for proMMP-9 could be seen. The *two lanes* on the *right* show reference signals for pure MMP-2 and proMMP-9

the rough surfaces and bone. On both rough surfaces, as well as on bone, bands of active MMP-9 was seen (82 kDa), however at a lower intensity than for proMMP-9 (92 kDa). A very weak band of proMMP-2 (72 kDa) was furthermore visible for TA, TLA and bone. Zymograms with cell lysates showed generally stronger bands but the observed differences between the groups were comparable on zymograms performed with cell lysates or supernatant. Non-activated osteoclasts which were cultured without RANKL showed no signals of MMP-2 or MMP-9 (data not shown).

4 Discussion

This study addresses the question of how osteoclasts interact and respond to titanium surfaces with increasing surface roughness, in comparison to their behavior on their native substrate, bone, which was used as a reference for intact osteoclast formation and activity. It was shown that RAW 264.7 cells adhere and differentiate into multinucleated TRAP-positive cells on all the examined surfaces; however, the individual response was dependent on the examined substrates. Generally, the most evident variation was observed between the smooth TS surface and the rough surfaces, TA and TLA. While proliferation was extensively promoted on TS and cells additionally showed a high TRAP activity, only few multinucleated cells were found on these surfaces compared to the rough titanium surfaces, confirming the findings of an earlier study [4]. Conversely, the increase in surface roughness between TA and TLA did not seem to have an influence on either TRAP activity or the number of osteoclasts. TRAP is an osteoclast marker enzyme that is proposed to be directly related to osteoclast resorption activity [29, 30]. On bone, a large number of osteoclasts were observed, accompanied by a significantly higher TRAP activity compared to that found

on titanium surfaces. This might be associated with biochemical signals present on bone but absent on titanium or could be a consequence of the fact that osteoclastic resorption does not take place on titanium but on bone where the resorption apparatus of the cells is fully established [31]. The cell number was additionally lower on bone than on titanium surfaces, suggesting that a higher fraction of RAW 264.7 cells might be activated to differentiate into multinucleated osteoclasts when grown on bone.

Qualitative visualization of cell morphology and adhesion by CLSM and SEM exposed elementary differences between cells grown on the different substrates. In line with the findings above, the most remarkable differences were found for cells cultured on TS in comparison with the other three substrates. While cells cultured on TA, TLA and bone showed a relatively high number of osteoclasts and a high number of actin rings, only few osteoclasts were found on TS. On TS, multinucleated cells were extremely large—significantly bigger than on the other surfaces; on the rough titanium surfaces, osteoclasts were smaller in size than those found on bone, which was also confirmed by qualitative analysis.

On TS, adhesion involved extensive podosome and filopodia formation rather than actin ring formation. It is proposed that the nature of giant cells and their limited actin ring formation on TS surfaces is associated with the cells' inability to establish a firm attachment to the underlying surface related to a higher turnover and limited stability of actin rings on such smooth substrates, thereby making them less detectable within a limited time frame [10, 11]. Unexpectedly, these giant cells were highly TRAP-active compared to cells cultured on rough surfaces. It is questionable whether these cells are activated osteoclasts or possibly could be related to inflammation-triggering giant cells, which are frequently formed at implant surfaces and related to foreign-body reactions [32, 33]. Some earlier studies have reported increased levels of TRAP activity in foreign-body giant cells (FBGC) [32, 34], however, further analysis would be needed to specify the phenotype of differentiated RAW 264.7 cells on smooth titanium substrates to verify the nature of the high TRAP activity. Differentiated osteoclasts cultured on the rough titanium surfaces exhibited no such giant-cell formation; on the contrary, the cells were morphologically similar to osteoclasts found on native bone and were smaller in size. This might suggest that increasing surface roughness might ease cell adhesion and thereby result in smaller sized osteoclasts. This is further supported by the diminishing number of filopodia on the rough titanium surfaces in comparison to the number found on the smooth TS surface. An increase in filopodia formation has also been reported, upon decreasing the nano-roughness of titanium substrates [9]. It is widely acknowledged that the resorption activity of osteoclasts is dependent on the formation of the sealing zone (SZ) [5, 14, 15]. Actin rings occurred frequently on rough titanium and bone surfaces but were virtually absent on TS. This is consistent with a reported study, in which actin ring formation was found to be small, incomplete and short lived on smooth substrates while larger and stable actin rings were observed on nano-rough calcite crystals [10]. A significant increase in actin ring size between TA and TLA as well as between TA and bone was observed, however no difference was found between TLA and bone. It could be speculated that actin ring size on TA and TLA corresponds with the size of the surface features on these surfaces [28]. The activation of actin ring formation is related to bone resorption, although we were surprised that they formed frequently on rough titanium surfaces. This implies that micrometer-scale topographical features on titanium can, in contrast to the behavior on the smoother TS, induce a cellular response that activates the resorption apparatus of an osteoclast.

Expression and secretion of proteolytic enzymes is dependent on SZ formation and is regulated on multiple levels, proMMP-9 having been shown to be upregulated in osteoclasts upon differentiation with RANKL [22]. Confirming the presence of MMPs allows for additional validation of osteoclast activation and was assessed by gelatin zymography with cell lysates of 11-day-differentiated RAW 264.7 cells. The intensity of the proMMP-9 signal was much weaker on TS when compared to the signals detected on the rough TA and TLA surfaces and bone; however no difference between these three groups could be observed. In addition to proMMP-9, weak bands of active MMP-9 as well as very weak signals for proMMP-2 were detected in the zymograms for the rough titanium surfaces and bone.

The zymography data correlate with the results on actin ring formation presented above. TA, TLA and bone showed pronounced actin ring formation and the highest intensity level of MMPs in gelatin zymography when compared to the impaired actin ring formation and low intensity of MMPs on the smooth surface. This indicates that osteoclasts can be induced to activate the resorption apparatus by cues of rough titanium surfaces, without the biological recognition of the surrounding ECM.

Assuming that, in bone remodeling, osteoclasts and osteoblasts show a close interplay, called coupling, regulated through multiple signaling pathways [35], our results might help to explain why rough implant surfaces show more successful osseointegration then smooth implant surfaces [36–38]. While on smooth surfaces osteoclast differentiation seems impaired and the foreign-body reaction is likely to occur, osteoclast differentiation on micro-rough implant surfaces seems to be comparable with

differentiation on native bone. Successful osteoclast differentiation will attract osteoblasts, which, in turn, will then mineralize bone around the implant.

5 Conclusions

The present study investigated osteoclast response and activation on titanium surfaces with increasing surface roughness, and compared this behavior with that on native bone. Our analysis revealed that osteoclasts can be activated on rough titanium surfaces (TA and TLA) in a comparable way to the behavior observed on native bone, while cells cultured on smooth titanium surfaces formed giant cells without comparable activation of the resorption apparatus. Increasing surface roughness, however, only had a minor effect on osteoclast morphology, the differentiation and activation of osteoclasts being merely dependent on the presence of surface roughness and not further stimulated by increased roughness. In combination with clinical data, this might help to further understand osseointegration of an implant and in particular the difference in osseointegration behavior between smooth and rough implant surfaces.

Acknowledgments The authors would like to thank Dr. Ute Hempel (Dresden University of Technology) for providing the RAW 264.7 cells, Peter Zimmermann (University of Basel) for cutting the bone slices, Dr. Anne Greet Bittermann (ZMB, University of Zurich) for SEM support, Thommen Medical for a scientific fellowship for TH and Katharina Maniura (EMPA St. Gallen) and Melanie Burkhardt (ETH Zurich) for careful reading of the manuscript. We would like to pay a special tribute to our colleague, supervisor and co-author Heike Hall, who recently passed away after a long illness, for her kindness, her insights, and her significant contributions to this work.

References

1. Hadjidakis DJ, Androulakis II (2006) Ann N Y Acad Sci 1092:385–396
2. Ericsson I, Johansson CB, Bystedt H, Norton (1994) Clin Oral Impl Res 5(4):202–206
3. Junker R, Dimakis A, Thoneick M, Jansen JA (2009) Clin Oral Impl Res 20(s4):185–206
4. Marchisio M, Di Carmine M, Pagone R, Piattelli A, Miscia S (2005) J Biomed Mater Res B Appl Biomater 75(2):251–256
5. Palmquist A, Omar OM, Esposito M, Lausmaa J, Thomsen P (2010) J R Soc Interface 7(Suppl 5):S515–S527
6. Bigerelle M, Anselme K, Ruderman I, Hardouin P, Iost A (2002) Biomaterials 23(7):1563–1577
7. Kunzler TP, Drobek T, Schuler M, Spencer ND (2007) Biomaterials 28(13):2175–2182
8. Webster TJ, Ergun C, Doremus RH, Siegel RW, Bizios R (2001) Biomaterials 22(11):1327–1333
9. Park J, Bauer S, Schlegel KA, Neukam FW, von der Mark K, Schmuki P (2009) Small 5(6):666–671
10. Geblinger D, Addadi L, Geiger B (2010) J Cell Sci 123(9):1503–1510
11. Geblinger D, Zink C, Spencer ND, Addadi L, Geiger B (2011) J R Soc Interface. doi:10.1098/rsif.2011.0659
12. Costa-Rodrigues J, Fernandes A, Lopes MA, Fernandes MH (2011) Acta Biomater 8(3):1137–1145
13. Makihira S, Mine Y, Kosaka E, Nikawa H (2007) Dent Mater J 26(5):739–745
14. Destaing O, Saltel F, Géminard JC, Jurdic P, Bard F (2003) Mol Biol Cell 14(2):407–416
15. Jurdic P, Saltel F, Chabadel A, Destaing O (2006) Eur J Cell Biol 85(3–4):195–202
16. Luxenburg C, Geblinger D, Klein E, Anderson K, Hanein D, Geiger B, Addadi L (2007) PLoS ONE 2(1):e179
17. Väänänen K, Zhao H (2002) Osteoclast function In: Bilezikian JP, Raisz LG, Rodan GA (eds) Principles of bone biology, vol 1. Academic Press, San Diego, pp 127–139
18. Väänänen HK, Karhukorpi EK, Sundquist K, Wallmark B, Roininen I, Hentunen T, Tuukkanen J, Lakkakorpi P (1990) J Cell Biol 111(3):1305–1311
19. Nagase H, Woessner JF (1999) J Biol Chem 274(31):21491–21494
20. Snoek-van Beurden PA, Von den Hoff JW (2005) Biotechniques 38(1):73–83
21. Tezuka K, Nemoto K, Tezuka Y, Sato T, Ikeda Y, Kobori M, Kawashima H, Eguchi H, Hakeda Y, Kumegawa M (1994) J Biol Chem 269(21):15006–15009
22. Wittrant Y, Theoleyre S, Couillaud S, Dunstan C, Heymann D, Redini F (2003) Biochem Biophy Res Commun 310(3):774–778
23. Dougall WC, Glaccum M, Charrier K, Rohrbach K, Brasel K, De Smedt T, Daro E, Smith J, Tometsko ME, Maliszewski CR et al (1999) RANK is essential for osteoclast and lymph node development. Genes Dev 13 (18):2412–2424
24. Minkin C (1982) Calcif Tissue Int 34(1):285–290
25. Sheu T-J, Schwarz EM, Martinez DA, O'Keefe RJ, Rosier RN, Zuscik MJ, Puzas JE (2003) J Biol Chem 278(1):438–443
26. Hsu H, Lacey DL, Dunstan CR, Solovyev I, Colombero A, Timms E, Tan HL, Elliott G, Kelley MJ, Sarosi I (1999) Proc Natl Acad Sci USA 96(7):3540–3545
27. Collin-Osdoby P, Yu X, Zheng H, Osdoby P (2003) In: Helfrich MH, Ralston SH (eds) Bone Research Protocols, vol 80. Humana Press, Totowa, pp 153–166
28. Hefti T, Frischherz M, Spencer ND, Hall H, Schlottig F (2010) Biomaterials 31(28):7321–7331
29. Kirstein B, Chambers TJ, Fuller K (2006) J Cell Biochem 98(5):1085–1094
30. Halleen JM, Alatalo SL, Suominen H, Cheng S, Janckila AJ, Väänänen HK (2000) J Bone Miner Res 15(7):1337–1345
31. Lutter A-H, Hempel U, Wolf-Brandstetter C, Garbe AI, Goettsch C, Hofbauer LC, Jessberger R, Dieter P (2010) J Cell Biochem 109(5):1025–1032
32. Kadoya Y, Al-Saffar N, Kobayashi A, Revell P (1994) Bone Miner 27(2):85–96
33. Neale SD, Athanasou NA (1999) Acta Orthop 70(5):452–458
34. Janckila AJ, Slone SP, Lear SC, Martin A, Yam LT (2007) Am J Clin Pathol 127(4):556–566
35. Parfitt AM (2000) Bone 26(4):319–323
36. Mangano C, Perrotti V, Iezzi G, Scarano A, Mangano F, Piattelli A (2008) J Oral Implantol 34(1):17–24
37. Buser D, Nydegger T, Oxland T, Cochran DL, Schenk RK, Hirt HP, Snétivy D, Nolte L-P (1999) J Biomed Mater Res 45(2):75–83
38. Boyan BD, Schwartz Z, Lohmann CH, Sylvia VL, Cochran DL, Dean DD, Puzas JE (2003) J Orthop Res 21(4):638–647